)05) 061111.
l. Acad. Sci. U.S.A., **106**

netry: An Introduction

1) 173.
006) 1741.

h. Appl., **12** (1986) 641.
hys., **104** (2008) 033504.
41113.
)05) 7854.
ev. B, **50** (1994) 1988.
ucture and Macroscopic

E, **74** (2006) 061308.
; C. M., *Phys. Rev. Lett.*,

HORPE M. F., *Phys. Rev.*

IHARDT P. J., *Phys. Rev.*

Proceedings of the International School of Physics "Enrico Fermi"
Course CLXXIII "Nano Optics and Atomics: Transport of Light and Matter Waves", edited by R. Kaiser, D. S. Wiersma and L. Fallani
(IOS, Amsterdam; SIF, Bologna)
DOI 10.3254/978-1-60750-755-0-51

Diffuse optics: Fundamentals and tissue applications

R. C. MESQUITA and A. G. YODH

Department of Physics & Astronomy, University of Pennsylvania
209 South 33rd Street, Philadelphia, PA 19104-6396, USA

Summary. — The material in this paper is different from the mainstream topics in this summer's International School of Physics "Enrico Fermi". It should become apparent, however, that the roots of these biomedical optics research problems share common features with much of the light scattering and transport research taught in the Varenna summer school. Here, our intention is to provide an informal review that establishes the roots of diffuse optics, and then demonstrates how diffuse optics is finding application in medicine. This paper will have two main themes. After a brief motivation of the problem, the first theme will provide a coherent discussion about light transport in turbid media. The second theme is oriented towards problems in biomedicine. As such, a short discussion of hemodynamics will be followed by representative current work from our lab, particularly with breast and brain.

1. – Introduction

The dream of optics for *in vivo* biopsy has been with us in various contexts for many years, and it continues to pop up in popular culture, particularly science fiction. Famous examples come from the TV show *Star Trek*, wherein Dr. McCoy uses a "tricorder" device to assess the condition of a patient, and from movies such as *Minority Report*, wherein fiber optics pick up brain signals from special patients. In most cases, an instrument

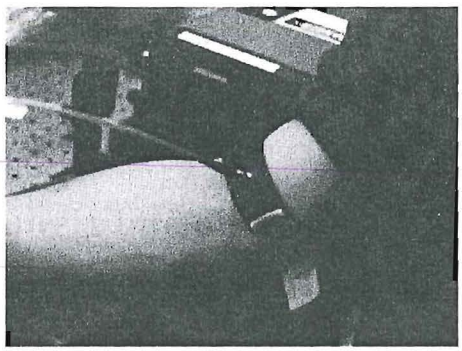

Fig. 1. – Illustration of a diffuse optical measurement on a subject's arm. One source fiber and one detector fiber are shown, separated by approximately 2 cm.

shines light into the body and/or collects light from the body in transmission or reflection; then a scientist employs the data to make a rapid diagnosis.

Without thinking too hard about the details, one might believe that such measurements are possible. For example, if we use light in the near-infrared (700–950 nm) rather than the uv, visible or mid- and far-infrared parts of the spectrum, then human tissue has a window of low absorption. Within this window, the absorption of oxy- and deoxy-hemoglobin is falling to zero, and the absorption of water has not started to increase significantly. Thus, light from such near-infrared devices can penetrate deeply in tissue. Furthermore, since each tissue chromophore has distinct spectral features, one can readily envision using light transmission properties as a function of wavelength to acquire sensitivity to tissue physiology, particularly to blood dynamics and edema. It has thus turned out that, besides the obvious convenience of such a device for continuous non-invasive measurement at the bedside, optical contrasts are complementary to other kinds of medical diagnostics such as, for example, X-ray and ultrasound.

A typical diffuse optical measurement is shown in fig. 1. This image reveals what we mean by "deep tissue", *i.e.*, big chunks of tissue located millimeters to centimeters below the tissue surface. Typically an optical fiber, coupled to a light source such as a diode laser, injects light into the tissue at the air-tissue interface, and a second optical fiber collects remitted or transmitted light at another position on the air-tissue surface. In practice, we vary source-detector position, light wavelength, light modulation, and even the mode of light detection in order to derive physiological information about the tissue in real time.

Currently, two limiting versions of this basic scheme are employed. One approach is diffuse optical imaging. In this case, many source-detector pairs are placed on the tissue surface, and the scientist attempts to reconstruct images of optical and physiological properties in each of many volume elements (or voxels) within the tissue interior based on measurements at the tissue surface. This imaging or tomographic scheme has been particularly prevalent in breast imaging. The second approach is tissue monitoring.

Here, a probe with few source-detector pairs is typically placed on (or near) tissues of interest, and average properties of the underlying tissues are derived by fitting reflection/transmission data to simple light diffusion models. This monitoring approach has been employed extensively in clinical studies of brain, muscle and tumor.

2. – Light transport tools

We now begin our discussion of light transport in tissues. In particular, we will introduce key physical and physiological parameters, and we will discuss important underlying concepts. We aim to facilitate understanding of the light diffusion problem in tissues, with minimal use of mathematics. Readers interested in more formal discussions can consult a variety of recent reviews [1-6] and references therein; a rather complete review from our group, *i.e.*, one that fleshes out the mathematics of many topics to be discussed herein, should be available soon in the journal *Reports on Progress in Physics.*

The natural starting point for our discussion is the optically thin or single-scattering sample. Typically such samples consist of molecules that can absorb light, and relatively larger particle-like objects that scatter light significantly. In the typical "traditional optics" experiment, the sample is illuminated with an incident light field (or incident light intensity), and we are concerned with how much light remains in the beam after the light traverses a distance L straight through the sample.

2˙1. *Absorption.* – The best known attenuation effect from traditional optics is light absorption (fig. 2a). Absorption is due to molecular chromophores in the sample and is characterized by an absorption coefficient, μ_a. The classic result for a transmission experiment of this kind is a law which states that the input light intensity is attenuated exponentially with distance traveled through the sample. The absorption coefficient that characterizes this attenuation depends on the concentration of chromophores in the sample and the chromophore cross-section or extinction coefficient —which in turn depends on incident-light wavelength. Thus, by carrying out such an absorption measurement as a function of input wavelength, one can learn which molecules are present, how many molecules reside in the sample, and one can even learn very subtle details about the molecule's local environment via spectral shifts or spectral broadening. In the case of tissue optics in the near infrared, the most important endogenous molecules are oxy- and deoxy-hemoglobin, water and lipid.

2˙2. *Scattering.* – A second important effect in traditional optics is scattering [7] (fig. 2b). The scattering effect is characterized by several variables. The first parameter, by analogy with absorption, is the scattering coefficient, μ_s, which is essentially the exponential decay rate of light intensity with distance traveled in the sample due to scattering effects. The scattering coefficient depends on the concentration of scattering particles and on the total scattering cross-section of these particles. This total scattering cross-section is generally wavelength-dependent (*e.g.*, depending on the particle size, the particle index of refraction, and on light wavelength), although the scattering cross-section usually has a much weaker wavelength dependence than typical molecular

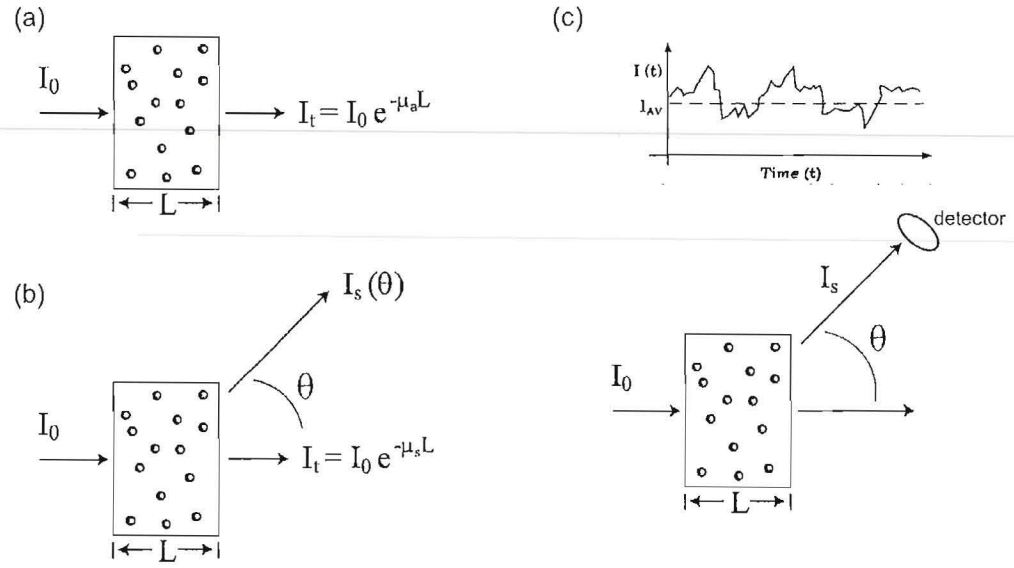

Fig. 2. – Schematic representation of different effects that light encounters when traversing an optically thin sample: (a) absorption, (b) scattering, and (c) dynamic scattering.

absorption spectra. Scattering experiments, however, can offer more information to the experimenter. Though the incident light is not transmitted, it is also not lost. Rather, it is sent off into different angular directions. This angular information can be measured and is quantified by the so-called differential scattering cross-section (or scattering amplitude). Note that the integral of the differential scattering cross-section over all angles equals the total scattering cross-section. The amount of light scattered into a particular solid angle is thus proportional to the product of the incident light beam intensity and the differential scattering cross-section at that angle.

Another factor that will eventually become of interest to us is the so-called anisotropy factor, g. The anisotropy factor is the average value of the cosine of the scattering angle for a typical scattering event. If the anisotropy factor, g, is near unity, then light scattering is nearly forward. If the anisotropy factor is about one half, then scattering is fairly isotropic and each scattering event is said to randomize the initial photon direction.

We introduce one more term in this context, because it turns out to be critical for light diffusion: the reduced scattering coefficient, μ_s'. The reciprocal of the reduced scattering coefficient is called the photon random walk step or transport-mean-free pathlength; after the incident light beam travels a photon random walk step in the scattering medium, only e^{-1} of the input light remains in the incident beam. The reduced scattering coefficient is simply related to the scattering coefficient and the anisotropy factor: $\mu_s' = \mu_s(1-g)$. The reduced scattering coefficient is the microscopic tissue scattering parameter that survives the diffusion approximations to the linear transport equation, which will be discussed shortly.

Scattering measure
cause substantial light
polystyrene, silica, PM
nucleus, etc.), and cell
scatterer concentration
of refraction affect scat
the case of absorption,

2·3. *Dynamic light s*
is called dynamic or qu
In these experiments, t
measured as a functio
their temporal autocor
ers. In particular we c
are moving, and in wh
typical dynamic light s
light from the sample a
propagation direction.
scatterers, and we shal
light field these particle
dipoles behave as ante
particle-like objects mo
at the detector will va
and destructively, depe
tal detected electric fie
are readily observed. T
carry information about
information about the n
poral autocorrelation fu
intensity autocorrelatio
of the autocorrelation fu
autocorrelation function
ticle mean-square displa
angle, and the incident
decay by e^{-1} when the

2·4. *Multiple light sc*
traditional optics probe
nential attenuation of th
even more about the na
quantities such as the t
are rigorous and have be

Tissues are more com
scatter light. One can e

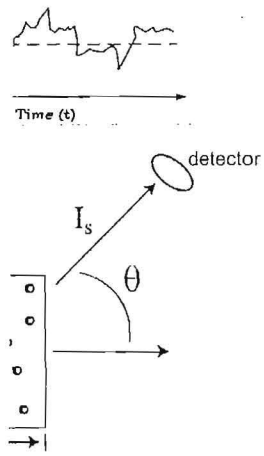

nters when traversing an
scattering.

ıore information to the
ɜ also not lost. Rather,
ıation can be measured
:tion (or scattering am-
s-section over all angles
ıttered into a particular
ght beam intensity and

the so-called anisotropy
:osine of the scattering
is near unity, then light
ɜ half, then scattering is
initial photon direction.
ıut to be critical for light
ɔf the reduced scattering
an-free pathlength; after
scattering medium, only
ɛd scattering coefficient
factor: $\mu_s' = \mu_s(1-g)$.
ıttering parameter that
equation, which will be

Scattering measurements such as this teach us about the microscopic objects that cause substantial light scattering. Examples of such objects include particles (*e.g.*, polystyrene, silica, PMMA, nanoparticles, etc.), cell organelles (*e.g.*, the mitochondria, nucleus, etc.), and cells (*e.g.*, red blood cells, etc.). In principle one can learn about scatterer concentration, about the fluids that surround the scatterers and whose indices of refraction affect scattering strength, and more. This information is very useful, as was the case of absorption, and it is complementary to the absorption information.

2˙3. *Dynamic light scattering.* – The final traditional optics topic that we will describe is called dynamic or quasi-elastic light scattering (*i.e.*, DLS or QELS, respectively) [8-10]. In these experiments, the fluctuations of scattered light intensity (or electric field) are measured as a function of time (fig. 2c). By analyzing these fluctuations, specifically their temporal autocorrelation functions, we can learn about the motions of the scatterers. In particular we can learn about how fast these particles are moving, how many are moving, and in what manner they are moving (*e.g.*, diffusive, ballistic, etc.). In the typical dynamic light scattering (DLS) experiment, a point-like photon detector collects light from the sample at an off-axis angle, *i.e.*, an angle different from the input beam propagation direction. The DLS effect is relatively easy to understand for particle-like scatterers, and we shall adopt this approximation here. In the presence of the input light field these particles acquire an oscillating induced-dipole moment. These oscillating dipoles behave as antennas and re-radiate light into many off-axis angles. When the particle-like objects move, the relative phases of these re-radiated dipole fields landing at the detector will vary too, and the re-radiated fields will add both constructively and destructively, depending on the particle configuration in the sample. Thus the total detected electric field (and intensity) will vary in time, and intensity fluctuations are readily observed. These fluctuations of the electric field strength and light intensity carry information about the dynamic properties of the medium. Specifically, they carry information about the mean-square displacements of the particles. The normalized temporal autocorrelation function of the scattered electric field, or the analogous temporal intensity autocorrelation function, is measured in the DLS experiment. The decay rate of the autocorrelation function depends on the particle motion; larger motions give faster autocorrelation function decay rates. Quantitatively, the decay rate depends on the particle mean-square displacement (during the autocorrelation time interval), the scattering angle, and the incident light wavelength. Often, the DLS autocorrelation function will decay by e^{-1} when the particles move a distance of about one optical wavelength.

2˙4. *Multiple light scattering in tissues.* – We have seen that the basic techniques of traditional optics probe both scattering and absorption, and both effects lead to exponential attenuation of the incident beam. Furthermore, the scattered beam can teach us even more about the nature of the scatterer and its motions, *e.g.*, if we measure other quantities such as the temporal autocorrelation function. These traditional techniques are rigorous and have been tested to a very substantial degree. The methods work.

Tissues are more complicated. Tissue samples are not optically thin. Tissues multiply scatter light. One can envisage the transport of photons through tissue as a sequence

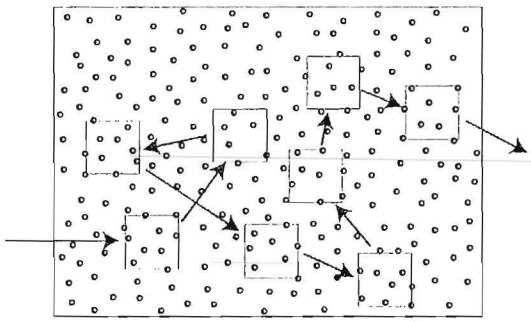

Fig. 3. – Pictorial representation of a light path due to multiple scattering in tissue.

of single scattering events (fig. 3). The light traverses the sample like a random walker. Incident light travels some distance into the sample and then scatters, and then it travels some distance along its new propagation direction and scatters again, and so on —many times over before it eventually emerges from the sample. In this case, absorption, scattering and correlation effects are seemingly scrambled together. Furthermore, the total pathlength travelled by the incident light is many times the sample size. Thus, if we want to learn something about these media, then we have to learn how to unscramble this information from the emerging light fields.

The use of Maxwell's full electromagnetic theory to address such a complex problem, in general, is extraordinarily difficult [11]. Fortunately, there exists a useful approximation called *linear transport theory*, which can deal with many aspects of the light transport problem in highly scattering media [12, 13]. Linear transport theory is not a perfect theory for the problem. For example, it ignores most (but not all) of the wave aspects of the light fields. However, it turns out that the theory provides a very useful starting point for many problems of light propagation in tissues. The key physical quantity in the theory is called the *radiance*. The radiance is basically the light power per area per solid angle at position $\mathbf{r}$ and time t in the sample, traveling in a particular direction, $\mathbf{\Omega}$. The radiance scales as the absolute square of the light field at $\mathbf{r}$, t and traveling in direction $\mathbf{\Omega}$. Linear transport theory balances the radiance in each small volume of the multiply scattering medium. This balance produces an equation for radiance, *i.e.*, the transport equation, that can, in principle, be used to solve for radiance throughout the sample given some spatio-temporal distribution of absorption and scattering coefficients, some distribution of differential scattering cross-section, boundary conditions, and initial conditions. Of course, the equation is non-trivial to solve, and closed-form solutions only exist for very simple geometries and conditions.

The physics behind the mathematics in linear transport theory becomes more evident within a first-order approximation of the radiance balance equation. In this case the diffusive nature of light transport becomes apparent. We will briefly outline some of the steps involved in going from the fully general transport equation to the light diffusion equation. In this regime, the two simplest and most important physical quantities associ-

ated with the radianc
at position $\mathbf{r}$ is a scal
centered on $\mathbf{r}$. It is th
photon flux is also de
in this case it is derive
nature of the radianc
the radiance.

To solve the transp
tion. In the P_N appro
scattering function ar
nomials. These expan
of equations of differe
show that the fluence
the flux depends only
i.e., in the so-called P
the radiance can be e
little more work, the t
fluence rate. We write

(1) $\nabla \cdot (D$

Here $\Phi(\mathbf{r}, t)$ is the ph
medium (cm/s), and
number of photons e
(Joules/cm^3 s). The n
cient D (cm^2/s); $D(\mathbf{r})$
the reduced scattering
The analysis also show
the fluence rate, as in

We therefore arriv
at this point to consid
which we have glossed
less than the absorptio
of tissues. Second, we
the flux; this approxi
and sources. We have
long as we do not ma
have assumed that th
on incident angle, *i.e.*
output wave vectors.
been made, which amo
longer than the time

ated with the radiance are the *photon fluence rate* and the *photon flux*. The fluence rate at position $\mathbf{r}$ is a scalar function derived by integrating the radiance over a small sphere centered on $\mathbf{r}$. It is the isotropic part of the radiance. The photon flux is a vector. The photon flux is also derived from an integration of the radiance over the solid angles, but in this case it is derived from a vector integration that takes explicit account of the vector nature of the radiance. The photon flux is the lowest-order anisotropic contribution to the radiance.

To solve the transport equation, typically one carries out the so-called P_N approximation. In the P_N approximation the radiance, the source distribution, and the differential scattering function are all expanded in terms of spherical harmonics or Legendre polynomials. These expansions are then stuffed back into the transport equation and a set of equations of different order are thus derived. Interestingly, it is straightforward to show that the fluence rate depends only on the zeroth-order spherical harmonic, and the flux depends only on the first-order spherical harmonics. Thus, in the lowest order, *i.e.*, in the so-called P_1 approximation where the expansions are truncated at first order, the radiance can be expressed precisely in terms of the fluence rate and flux. With a little more work, the transport equation reduces to the photon diffusion equation for the fluence rate. We write out the photon diffusion equation in its full glory below:

$$\nabla \cdot (D(\mathbf{r})\nabla\Phi(\mathbf{r},t)) - v\mu_a(\mathbf{r})\Phi(\mathbf{r},t) + vS(\mathbf{r},t) = \frac{\partial\Phi(\mathbf{r},t)}{\partial t}. \tag{1}$$

Here $\Phi(\mathbf{r},t)$ is the photon fluence rate (Joules/cm^2 s), v is the velocity of light in the medium (cm/s), and $S(\mathbf{r},t)$ represents an isotropic source term proportional to the number of photons emitted (at point $\mathbf{r}$ and time t) per unit volume per unit time (Joules/cm^3 s). The main new parameter in the problem is the photon diffusion coefficient D (cm^2/s); $D(\mathbf{r}) = v/3(\mu_s' + \mu_a)$, and (for small absorption) it depends primarily on the reduced scattering coefficient, the reciprocal of which is the photon random walk step. The analysis also shows explicitly that the photon flux is proportional to the gradient of the fluence rate, as in standard diffusion problems.

We therefore arrive at the key mathematical result of this paper. It is worthwhile at this point to consider some of the assumptions that went into this analysis, many of which we have glossed over. First we assumed that the scattering length, $(\mu_s)^{-1}$, is much less than the absorption length, $(\mu_a)^{-1}$, an assumption that is fine for the vast majority of tissues. Second, we implicitly assumed that the fluence rate is significantly larger than the flux; this approximation is generally fine, but it can break down near boundaries and sources. We have assumed isotropic sources, an assumption that is reasonable as long as we do not make measurements within a random walk step of the source. We have assumed that the scattering angle of a typical scattering event does not depend on incident angle, *i.e.*, it depends only on the cosine of the angle between input and output wave vectors. Finally, an assumption about the rate of change of the flux has been made, which amounts to requiring that the time scale of source modulation is much longer than the time between photon scattering events. Generally these assumptions

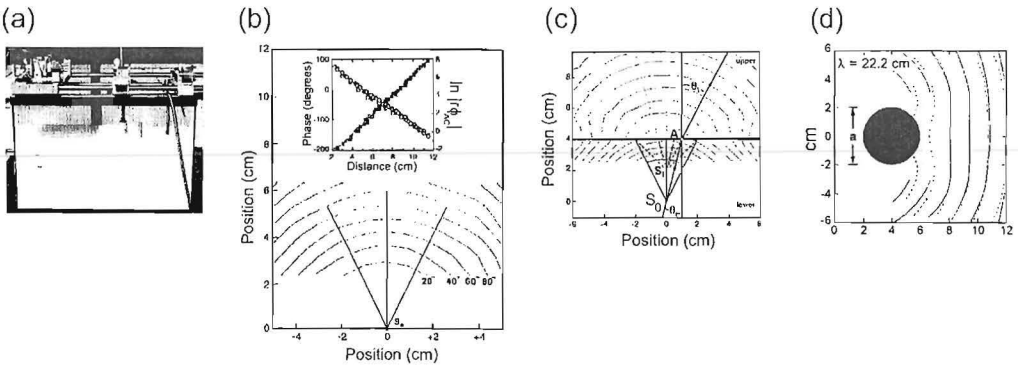

Fig. 4. – (a) Experimental setup for measurements in "ideal" turbid media, an aquarium filled with milky Intralipid. A source fiber injects light into the medium near its center, and a movable detector fiber measures amplitude and phase of the diffusive waves at different positions in sample. (b) Constant phase contours of diffusive wave in the aquarium. Notice, the contours are circular and emanate from the source. Inset: Measured phase and amplitude (in logarithm) as function of the source-detector separation. (c) Propagation through two different media; the medium containing source (S_0) has larger scattering then the other medium. Refraction effects are demonstrated. (d) Diffraction/scattering of diffusive wave due to an absorbing sphere of diameter a in the turbid medium [14, 15].

are fine for tissues. The photon random walk step in most tissues is about 1 mm and the absorption lengths are on the order of 5 to 10 cm. It is important, however, that our applications do not demand great precision from our measurements, otherwise the affects of so many relatively innocuous approximations can wash out the effects of the physiological perturbations we seek to probe.

2·5. *Simple solutions of the photon diffusion equation.* – In order to use the diffusion equation for light, we must understand its solutions. We start with ideal case of infinite, homogenous, turbid media. A good example of such a medium is an aquarium full of milk (or Intralipid) and ink (see fig. 4a). This kind of tissue phantom sample can be adjusted to have properties similar to tissues, without the clinical complications. Working in the frequency domain, the source is amplitude-modulated at some frequency ω (*e.g.*, 100 MHz), and we look for solutions that oscillate at this same frequency. In this case, the diffusion equation reduces to a very simple standard differential equation which will give spherical wave solutions with a complex wave number that depends on sample absorption and scattering, and on source modulation frequency. For a point oscillating source, the solution to this differential equation is the Green's function of the diffusion equation for the infinite homogenous geometry. Notice (in fig. 4b insets) that the wave attenuates exponentially with distance from the source, and that the phase of the wave disturbance has an associated wavelength that depends on scattering, absorption and frequency. The fundamental photon density disturbance is thus a kind of overdamped wave. We call these disturbances diffuse photon density waves, or diffusive waves. It

turns out that these di
regular waves we know
and medium effective i
walk step.

Some examples of n
and detectors in an aqu
experiments, one sourc
diffusive wave) modulat
todetector measures th
in the sample. In fig. 4
amplitude variation wit
absorption and reduced
we divide the tank into
type effects are apparer

Thus far we have us
problem in simple turb
In this case, we seek t
very short duration pu
whose terminal slope is
primarily to the light d

At this point it is w
gained. We now have a
turbid media by measu
by measuring the temp
we can derive the absc
even though the mediu

3. – Diffuse Optical

We first consider pi
practice is the semi-inf
To make progress on th
the interface. The bou
coming into the mediu
is traveling outward at
so-called partial flux bc
to its gradient at the sa
a length which can be e
the surrounding mediu
flux boundary conditio
nocuous approximation
extrapolated zero-boun
placed by a zero-bound

(d)

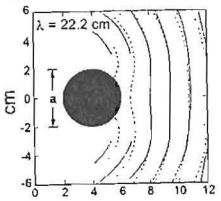

nedia, an aquarium filled
its center, and a movable
at different positions in
ım. Notice, the contours
amplitude (in logarithm)
ı two different media; the
edium. Refraction effects
o an absorbing sphere of

ɜues is about 1 mm and
ıportant, however, that
ırements, otherwise the
ɜh out the effects of the

rder to use the diffusion
ith ideal case of infinite,
um is an aquarium full
ue phantom sample can
e clinical complications.
ılated at some frequency
ɜ same frequency. In this
fferential equation which
that depends on sample
y. For a point oscillating
function of the diffusion
4b insets) that the wave
ıat the phase of the wave
attering, absorption and
us a kind of overdamped
ɛs, or diffusive waves. It

turns out that these disturbances of light energy density behave in many ways like the regular waves we know and love, except that properties such as disturbance wavelength and medium effective index of refraction depend on factors such as the photon random walk step.

Some examples of measurements we made to confirm these ideas using point sources and detectors in an aquarium filled with Intralipid and ink are given in fig. 4b-d. In these experiments, one source fiber is employed to launch a diffuse photon density wave (or diffusive wave) modulated at 200 MHz into the medium. Another fiber coupled to a photodetector measures the phase and amplitude of the diffusive wave at different positions in the sample. In fig. 4b, one can see a nice spherical diffusive wave, whose phase and amplitude variation with respect to source-detector separation can be used to obtain the absorption and reduced scattering coefficients of the turbid medium. In the third figure we divide the tank into two media with differing photon random walk steps. Refraction type effects are apparent in this case. The last figure shows diffraction/scattering effects.

Thus far we have used a frequency domain picture to analyze the light propagation problem in simple turbid media. We can also solve the problem in the time domain. In this case, we seek the Green's function solutions due to a point source emitting a very short duration pulse in the infinite media. The result is a broadened light pulse whose terminal slope is related to sample absorption and whose peak position is related primarily to the light diffusion coefficient in the sample.

At this point it is worth reflecting on what has been gained. In fact, a lot has been gained. We now have an experimental means to separate scattering from absorption in turbid media by measuring the phase and amplitude of diffuse photon density waves or by measuring the temporal broadening of a very short light pulse in the medium. Thus we can derive the absorption coefficient and the scattering properties of the medium, even though the medium is turbid. Next we explore the effects of heterogeneity.

3. – Diffuse Optical Spectroscopy (DOS): monitoring

We first consider piecewise continuous turbid media. A most important example in practice is the semi-infinite medium, *e.g.*, a tissue medium with an air-tissue interface. To make progress on this problem, we need boundary conditions for the fluence rate at the interface. The boundary condition is simple to state. We require that the radiance coming into the medium at the boundary is equal to the Fresnel reflected radiance that is traveling outward at the boundary. The result of carrying out this analysis is the so-called partial flux boundary condition, which relates the fluence rate at the boundary to its gradient at the same boundary. The proportionality constant in this relationship is a length which can be explicitly derived and which depends on the indices of refraction of the surrounding medium. One can solve the light diffusion problem exactly with partial flux boundary conditions (for the semi-infinite medium), or one can invoke a fairly innocuous approximation which leads to an even simpler boundary condition: the so-called extrapolated zero-boundary condition. In this case, the true boundary condition is replaced by a zero-boundary condition at an extrapolated distance L_s above the boundary,

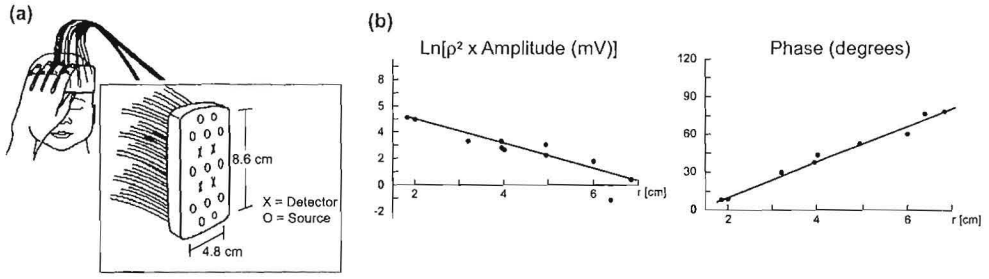

Fig. 5. – (a) Schematic showing the probe on the baby and the probe with its sources (o) and detectors (×). (b) Measured amplitude and phase as a function of separation for different source-detector combinations (black dots). The line in both plots represents the best fit to the data points, and the slopes can be used to derive tissue absorption and scattering coefficients [16].

i.e., the fluence rate vanishes at the extrapolated distance. The zero-boundary condition problem can then be solved by the classic method of images to derive a simple result for the predicted diffuse light reflectance from a semi-infinite turbid medium.

Believe it or not, this light reflectance result for semi-infinite homogeneous turbid media is THE workhorse result of the *monitoring* field. It performs fairly well in the clinic, giving average optical properties quite accurately, even though the media are not truly homogeneous or semi-infinite. As an example, fig. 5 shows a measurement of the optical properties of a baby brain. We used a pad with many sources and detectors, and placed it on the baby's head. Then we measured the diffuse photon density wave amplitude and phase as a function of source-detector separation. A fit to the data using the extrapolated zero-boundary condition provides the average tissue scattering and absorption coefficients at a single optical wavelength.

If the medium is slab-like instead of semi-infinite, it is straightforward to derive other analytic results. One can also derive results for cylinders, spheres, spheres in slabs, and more. We will not discuss these examples further. Suffice to say that for simple monitoring applications, some sort of analytic model can always be found to fit for measured phase and amplitude data, and, therefore, for deriving average scattering and absorption coefficients.

Before turning to imaging and tomography, we briefly consider the critically important problem of tissue diffuse optical spectroscopy (DOS). Thus far we have discussed the reflectance problem at a single optical wavelength. Arguably the most important feature of optics, however, is its potential for spectroscopy. For example, suppose we assume that there are two chromophores in tissue, oxy- and deoxy-hemoglobin; both of these chromophores will contribute to the measured absorption coefficient. The relative amount that each chromophore contributes depends on its extinction coefficient and its concentration. If we derive tissue absorption coefficients at multiple wavelengths —say 780 nm and 805 nm— then we generate two equations with two unknowns. The two unknowns are the concentrations of oxyhemoglobin ($[HbO_2]$) and deoxyhemoglobin ([Hb]).

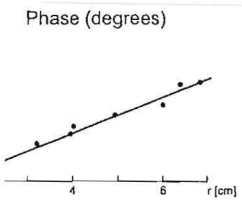

with its sources (○) and
ıtion for different source-
the best fit to the data
tering coefficients [16].

ro-boundary condition
rive a simple result for
medium.
e homogeneous turbid
ɔrms fairly well in the
ɔugh the media are not
a measurement of the
sources and detectors,
e photon density wave
ɔn. A fit to the data
erage tissue scattering

forward to derive other
ıeres, spheres in slabs,
to say that for simple
ıys be found to fit for
average scattering and

er the critically impor-
; far we have discussed
ɔly the most important
r example, suppose we
xy-hemoglobin; both of
coefficient. The relative
ction coefficient and its
tiple wavelengths —say
ınknowns. The two un-
eoxyhemoglobin ([Hb]).

By solving these equations, using the data and the known chromophore extinction coefficients, we can therefore derive $[HbO_2]$ and [Hb]. From this information we can further derive total hemoglobin concentration ($[THC] = [HbO_2] + [Hb]$) and tissue blood oxygen saturation ($S_tO_2 = [HbO_2]/([HbO_2] + [Hb])$). [THC] and S_tO_2 are important clinical quantities that can thus be derived from relatively simple multi-wavelength, diffuse optical reflectance measurements. These reflectance techniques go by the names Diffuse Optical Spectroscopy (DOS) or Near-Infrared Spectroscopy (NIRS) in the biomedical optics community.

4. – Diffuse Optical Tomography (DOT): imaging

Suppose the media we seek to understand are very heterogeneous. Furthermore, suppose that these heterogeneities are the quantities which we seek to learn about. How does one handle this situation? In this case, some kind of tomography or image reconstruction is desirable [17-19]. Fortunately, it is conceptually straightforward to develop strategies for this goal, because the heterogeneity problem is basically a problem that has already been studied in the context of waves and scattering theory. The only difference for us is that the waves are now diffuse photon density waves. In essence, in our experiments an incident diffusive wave is launched from each source fiber into the medium and the wave scatters from local optical property heterogeneities. From measurements of scattered waves on the tissue surface, one can set up an inverse problem to work backwards from the "perturbed" wave at the tissue surface to derive the heterogeneous optical properties within the entire medium.

The standard approach for setting up the problem is to divide the absorption and light diffusion coefficients into background and heterogeneous pieces, and then insert these parameters back into the diffusion equation. Then we look for perturbative solutions. Both the Born perturbation approach and the Rytov perturbation approach [20] will work as long as scattering of diffusive waves by heterogeneities in the sample is weak.

As a concrete example, let us suppose the tissue optical property variation is only due to absorption. In this case the scattered wave depends approximately on the value of the incident wave at the heterogeneity times the strength of the heterogeneity times a propagator that describes the diffusive wave transport from the heterogeneity to the detector. The propagator is just the Green's function for the diffusive wave.

Within this formulation, there will arise an integral equation for every source-detector pair on the sample surface. The integral is over the entire sample volume. At this point the sample volume is divided up into discrete-volume elements and the inverse problem is formulated readily in the language of matrices. Here, a weight matrix, whose elements are basically the product of Green's functions, couples a vector of tissue optical properties to a vector of measurements of the scattered diffusive waves. The absorption unknowns in each volume element of the sample are represented as a vector; the measured scattered signals for each source-detector pair are also represented by elements of a measurement vector. The result is a set of linear equations that can be inverted, for example, by the singular value decomposition technique [21], to derive an absorption tomogram. In

practice many other techniques can be used to solve this class of problems, though issues of uniqueness and regularization always crop up. Most people nowadays solve the inverse problem iteratively, a method of choice when the heterogeneities are not weak. DOT has been demonstrated to work very well in phantoms. Its use in the clinic is promising and is a subject of current research.

5. – Diffuse Correlation Spectroscopy (DCS): blood flow

We will discuss one last formal problem before moving to applications: Diffuse Correlation Spectroscopy (DCS). DCS is a multiple-scattering correlation methodology for measuring blood flow.

First, let us recall the single-scattering version of this problem: dynamic light scattering. In the DLS experiment, a sample is illuminated. Illuminated particles in the sample act like radiating dipoles. We collect their radiated fields with a photon detector located off at some scattering angle. The collected fields fluctuate and the intensity fluctuates too, because the particles move and the relative phases of the radiated dipole fields change as a result of this motion. Information about scatterer motions is contained in the electric field and intensity temporal autocorrelation functions. The electric field autocorrelation function decays exponentially at a rate that depends on how far the scattering particles move in the correlation time interval, *i.e.*, on the particles' mean-square displacement in the correlation time interval. Thus, we derive motional information by measuring this decay rate.

Several schemes can be employed to analyze this problem in the multiple scattering limit. To keep things formally consistent, we will focus on the transport equation methodology. Ackerson and coworkers [22, 23] suggested that it should be possible to understand the propagation of temporal autocorrelation in turbid (and dynamic) media primarily by replacing *radiance* in the transport equation with the *normalized electric field temporal autocorrelation function.* This replacement is tantamount to exchanging the function $E^*(\mathbf{r},t,\mathbf{\Omega})E(\mathbf{r},t,\mathbf{\Omega})$ in the transport equation with $E^*(\mathbf{r},t+\tau,\mathbf{\Omega})E(\mathbf{r},t,\mathbf{\Omega})$; here $E(\mathbf{r},t,\mathbf{\Omega})$ is the electric field of the diffusing light at $\mathbf{r}$, t and traveling in the direction $\mathbf{\Omega}$ (hereafter we will supress the propagation direction in our notation), and τ is the autocorrelation function time delay or interval. Then, following essentially the same logic and mathematics as before, we arrive at a linear transport equation for correlation, this time with the scattering source term that we have from DLS. We make the P_1 approximation, as before, to convert the correlation transport equation to the Correlation Diffusion Equation shown below [24, 25]:

$$\nabla\cdot(D(\mathbf{r})\nabla G_1(\mathbf{r},\tau)) - v\left(\mu_a(\mathbf{r}) + \frac{\alpha}{3}\mu_s' k_0^2\langle\Delta r^2(\tau)\rangle\right) G_1(\mathbf{r},\tau) = vS(\mathbf{r},t), \tag{2}$$

where $G_1(\mathbf{r},\tau) = \langle E^*(\mathbf{r},t+\tau)E(\mathbf{r},t)\rangle$ is the unnormalized temporal electric field autocorrelation function; k_0 is the wave vector of the fields in the medium, and $\langle\Delta r^2(\tau)\rangle$ is the mean-square displacement of the scattering particles in time τ. The brackets $\langle\ \rangle$

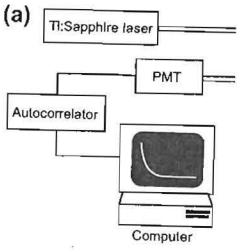

Fig. 6. – (a) Schemati
correlation curves mea
cuff pressure increases

denote ensemble ave
tion of scattering ev
source term.

The correlation d
autocorrelation! Noti
conventional diffusio
result (eq. (2)) is the
technique [26-28] tha
school. The differenti
all the formal ideas v
apply to diffusing fiel
diffusion equation ar
absorption term due t
imaging measuremen

Figure 6 shows an
The measurement of
and it gives an auto
increased, the slope o
can be used to define
function decay rate is
to an effective diffusi
parameterizes the cor
for the fraction of scat
changes in BFI, *i.e.*, r
flow changes in a broa

6. – Background or

Before we describe
call the tissue param
provides access to the

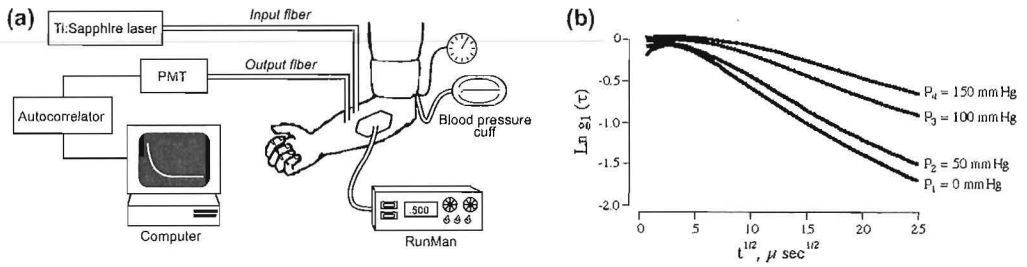

Fig. 6. – (a) Schematic diagram of the cuff ischemia experiment. (b) Intensity temporal autocorrelation curves measured for different cuff pressures. Notice that the decay rate decreases as cuff pressure increases, indicating attenuation of blood flow (obtained from [29]).

denote ensemble averages, or averages, over time. The parameter α represents the fraction of scattering events in the tissue that occur from moving particles, and $S(\mathbf{r})$ is a source term.

The correlation diffusion equation is a diffusion equation for electric field temporal autocorrelation! Notice that in the limit that τ goes to zero, this equation reduces to the conventional diffusion equation for fluence rate in the zero-frequency limit. Formally, this result (eq. (2)) is the differential equation form of the diffusing wave spectroscopy (DWS) technique [26-28] that Georg Maret invented and has also talked about in this summer school. The differential equation form is particularly attractive, however, because almost all the formal ideas we have discussed with respect to diffuse photon density waves will apply to diffusing field temporal autocorrelation. That is, the solutions of the correlation diffusion equation are formally the same as for fluence rate with only an additional absorption term due to particle motions. Thus, it follows that analogous monitoring and imaging measurements can be carried out with diffusing correlation.

Figure 6 shows an example of a blood flow measurement, based on cuff ischemia [29]. The measurement of correlation is carried out with source and detector on the forearm, and it gives an autocorrelation function that decays in time. As the cuff pressure is increased, the slope of the autocorrelation decay decreases. Thus the slope of this curve can be used to define a blood flow index (BFI) for clinical experiments. The correlation function decay rate is used to get the BFI. The BFI, in turn, can be related explicitly to an effective diffusion constant (not the Einstein Brownian Diffusion constant), that parameterizes the correlation function decay rate, times the factor alpha, which accounts for the fraction of scattering events from moving scatterers. We have found that relative changes in BFI, *i.e.*, rBFI, provide a robust and quite accurate measure of relative blood flow changes in a broad range of clinical scenarios [30-38].

6. – Background on tissue hemodynamics

Before we describe some physiological applications of diffuse optics, let us briefly recall the tissue parameters to which these tools are sensitive. Absorption information provides access to the tissue concentrations of endogenous chromophores such as HbO_2,

Hb, water and lipid, and also to the concentrations and local environments of exogenous chromophores such as imaging contrast agents and drugs. Scattering information provides access to organelle concentrations, cell concentrations, and subtle changes in the properties of background fluids. Correlation spectroscopy provides information about the movement and flow of scattering "objects" in tissues such as red blood cells. Taken together, the most prevalent application of these tools is for probing tissue hemodynamics. In this case, absorption gives information about total hemoglobin concentration and tissue blood oxygen saturation, and correlation spectroscopy gives information about blood flow down to the tissue microvasculature level. Of course, all of these measurements represent tissue-averaged quantities; the degree of tissue averaging depends on the source-detector geometry.

The circulatory system is a network of channels of varying diameter with the purpose to deliver nutrients to tissues and remove waste products of metabolism from tissues [39]. The arterial side of the vasculature is oxygen rich; it takes blood from heart and lungs to tissues. The venial side of the vasculature is oxygen poor; it takes blood back to the heart and lungs. The network is branched. The tubes start big, but break into smaller and smaller tubes until finally (at the oxygen delivery points), the capillaries bring red blood cells and plasma cells to within a hundred or so microns of every tissue cell in the body. The arterioles, capillaries and venules therefore fill up a very sizable fraction of the tissue space. Thus, it is their responses that we are typically measuring with diffuse optics. Each red blood cell carries many molecules of hemoglobin (oxygenated or deoxygenated), the primary oxygen carrier.

As we have noted, two forms of hemoglobin are important: oxygenated and deoxygenated. These hemoglobin molecules are typically in chemical equilibrium with dissolved oxygen in the tissue. When dissolved oxygen is low in tissue, then oxygen is unloaded off the HbO_2 molecules and then the oxygen diffuses into the tissue. This equilibrium between blood oxygen saturation and tissue pO_2 is characterized by the classic "Hill Curve" [39, 40]. Remember that diffuse optics measures blood oxygen saturation, which is closely related to tissue pO_2 via the Hill Curve.

When tissue oxygen is low, then bad things can happen to tissues. Briefly, oxygen is brought into tissues via the arterioles, and then some of this oxygen is used by the tissues for metabolic processes, and the leftover oxygen is removed via the venules. Hypoxia occurs when tissue oxygen is low. This condition can arise from a variety of effects. For example, the amount of breathed oxygen could be low (as on a high mountain), or the delivery of oxygen to the tissue could be impaired (*e.g.*, by blockages in the feeding arteries), or the tissue metabolism could be abnormally high, etc. Tissue hypoxia can therefore reflect problematic clinical scenarios such as ischemic stroke, therapy resistant hypoxic tumors, muscle disease, and more.

To recapitulate, tissue oxygen dynamics are important in clinical contexts. Diffuse optics does not measure pO_2 directly, but it does measure blood oxygen saturation, total hemoglobin concentration, and blood flow. All of these hemodynamic ingredients are useful to know, and they permit experimenters to develop a picture of the functioning (or malfunctioning) tissue. In fact, measurement of changes in all three hemodynamic

quantities permits s
erty: oxygen metabo
in all-optical functio
metabolism [31, 32].

7. – Validation an

We will use the re
from our laboratory
These examples are n
a review of all activit
kinds of measurement

We will begin with
as for many researche
For example, in fig. 7
partial pressure in tiss
a simple tissue phant
similar to those of hun
Over the course of sa
with needle electrodes
oxygen saturation with
be apparent that the c
optical HbO_2 and Hb
relative changes in DO
oxygen saturation) as a
carbogen breathing. W
Indeed there is a subst
of tissue blood oxygen
diagnostics and/or with

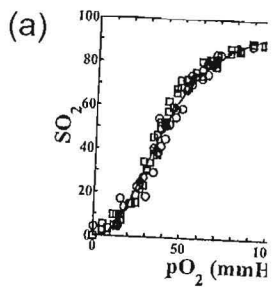

Fig. 7. – (a) Oxyhemoglob
phantom. (b) Correlation
diffuse optics, and relative
tumors in mice during carb

quantities permits scientists to compute changes in another fundamental tissue property: oxygen metabolism. Convincing recent work along these lines has been carried out in all-optical functional experiments in brain, which probe changes in cerebral oxygen metabolism [31, 32].

7. – Validation and clinical examples

We will use the remainder of this paper to provide a set of representative illustrations from our laboratory of the diffuse optical techniques in clinical and pre-clinical studies. These examples are not intended to be comprehensive; nor are they intended to provide a review of all activity in the field. Rather, they are intended to give a flavor for the kinds of measurements that are becoming possible.

We will begin with some validation studies. One goal for our research group (as well as for many researchers in biomedical optics) is to validate the diffuse optical methods. For example, in fig. 7a we show a measurement of the Hill Curve that relates oxygen partial pressure in tissue to blood oxygen saturation. The data in fig. 7a are derived from a simple tissue phantom experiment. The tissue phantom had optical properties very similar to those of human tissue and contained mouse erythrocytes (*i.e.*, mouse blood). Over the course of sample deoxygenation we measured both oxygen partial pressure with needle electrodes (both Eppendorf histograph and Clark-style electrodes) and blood oxygen saturation with a standard diffuse optical spectroscopy (DOS) set-up. It should be apparent that the curve behaves as expected, thereby providing validation for diffuse optical HbO_2 and Hb quantification. In fig. 7b, *in vivo* mouse tumor experiments show relative changes in DOS-measured S_tO_2 (in figure, S_tO_2 and SO_2 both refer to blood oxygen saturation) as a function of relative changes in Eppendorg histograph pO_2 during carbogen breathing. We see that the two techniques are again in quite good agreement. Indeed there is a substantial literature that corroborates DOS (NIRS) measurements of tissue blood oxygen saturation and blood volume concurrently with other medical diagnostics and/or with the literature.

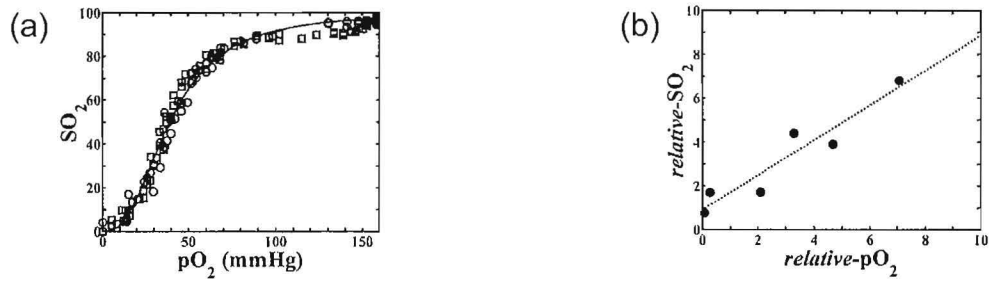

Fig. 7. – (a) Oxyhemoglobin dissociation curve obtained from mouse erythrocytes in a tissue phantom. (b) Correlation between relative blood oxygen saturation (SO_2), as measured by diffuse optics, and relative pO_2, as measured by an Eppendorf histograph, in fibrosarcoma tumors in mice during carbogen breathing [41].

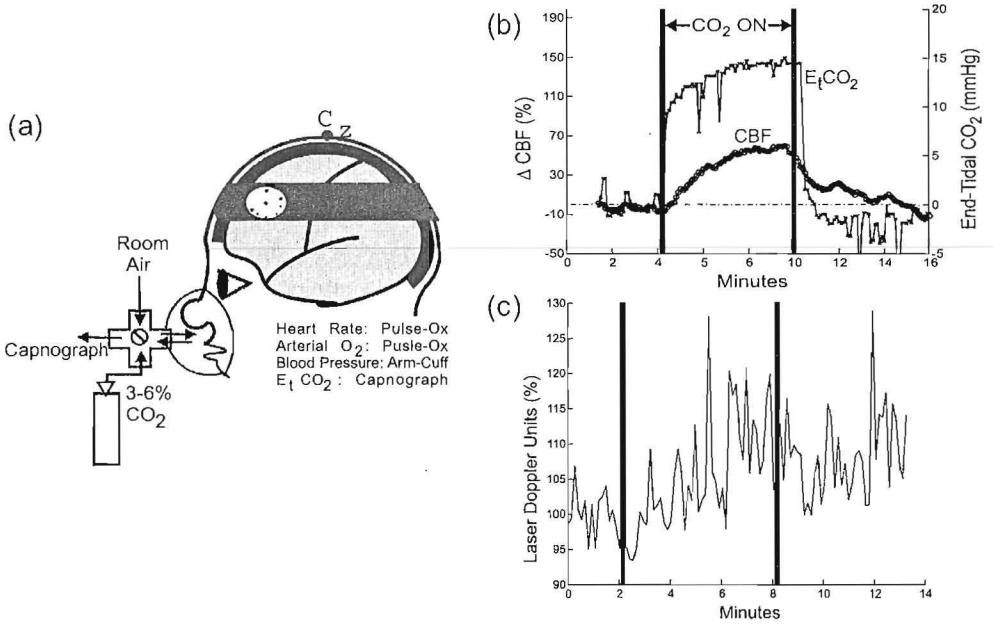

Fig. 8. – (a) Schematic diagram of the hypercapnia experiment. (b) Measured end-tidal CO_2 and CBF, from DCS, for a single subject. (c) Simultaneous skin/scalp flow measured by Laser Doppler for the same subject. Activation occurs between the thick solid lines in the figure.

Serious validation of diffuse correlation spectroscopy (DCS) has only begun relatively recently [32, 36, 38, 42, 43]. In fig. 8 we show the functional blood flow response of an adult to a hypercapnia perturbation [42]. In hypercapnia, the subject breathes excess CO_2 and blood flow is increased in his/her brain as a result. In practice we place the DCS probe (with source-detector separation of 2.5 cm on the tissue surface) locally on the head, even though hypercapnia is a whole-brain response. In DOS/DOT and DCS measurements, light penetration depth through the scalp and skull and into the cortex depends on source-detector separation; the penetration depth is typically one-third to one-half of the source-detector separation on the surface of the head. Thus, the light penetrates into approximately 0.5 cm of cortex in the present case. The increase in blood flow with inspired pCO_2 is evident from the data and is in quantitative agreement with other measurements from the literature [44-46]. We also confirmed that the DCS measurement is not simply measuring skin/scalp flow, by comparing the DCS response to the much smaller (and noisier) Laser Doppler skin/scalp flow measurement.

As a second DCS validation example, we show data from experiments in brain-injured patients in the neuro-intensive care unit [47]. In this case (fig. 9), we compared DCS measurements of cerebral blood flow to flow measurements by xenon-CT. The latter is a standard-of-care flow measurement in the clinic, but it cannot be used for continuous bedside monitoring because of its complexity. Using the Xe-CT images, we can compare

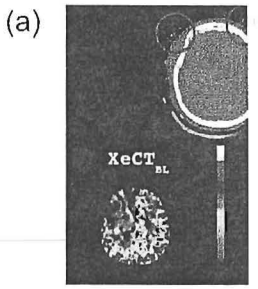

Fig. 9. – (a) Top: sing
probes outlined. Botto
XeCT scan. (b) Correl
for more details, see [47

the same tissue volun
sopressor drugs. A sir
and to follow respons
were quite strongly cc

Beyond validation,
tigation. The first cla
second class of study i
of each class.

First, we illustrate
have been developed t
with verbal fluency, v
classic motor stimuli
thumb against your f
cortex is activated.
hemodynamic respons
in vivo, through the s
multiple source-detect
DOS and DCS measur
subjects, sometimes w
sometimes over the a
away from this activat

Our observations a
place", activation was
over the motor activat
oxy-, deoxy-hemoglob
permits comparison w
the all-optical probe!

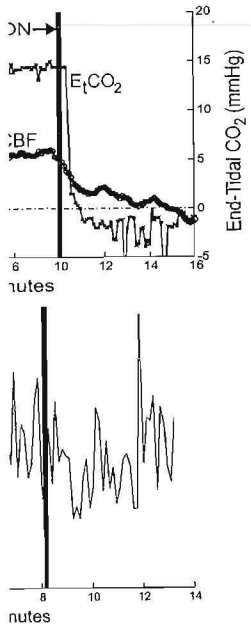

Measured end-tidal CO_2
flow measured by Laser
id lines in the figure.

is only begun relatively
od flow response of an
subject breathes excess
a practice we place the
sue surface) locally on
a DOS/DOT and DCS
ull and into the cortex
typically one-third to
head. Thus, the light
case. The increase in
quantitative agreement
onfirmed that the DCS
uring the DCS response
measurement.
iments in brain-injured
9), we compared DCS
enon-CT. The latter is
be used for continuous
mages, we can compare

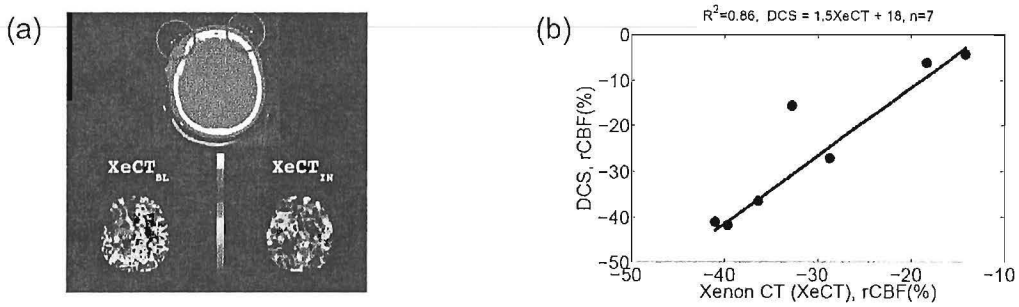

Fig. 9. – (a) Top: single axial slice from non-contrast CT scan, with the region under DCS probes outlined. Bottom: baseline (left) and after Xe infusion (right) CBF maps obtained from XeCT scan. (b) Correlation between CBF as measured by DCS and xenon CT (color online; for more details, see [47]).

the same tissue volumes during various drug stimulations, such as increased dose of vasopressor drugs. A simple protocol was thus set up to induce cerebral blood flow changes and to follow responses with both techniques. Again, we found that both techniques were quite strongly correlated (fig. 9) [47].

Beyond validation, research in the field is oriented towards two classes of brain investigation. The first class of study is concerned with the function of normal brain, and the second class of study is clinical, aimed to improve patient care. We will give one example of each class.

First, we illustrate functional imaging through the skull. Many functional paradigms have been developed to understand normal responses associated, for example, with vision, with verbal fluency, with motor skills, and more. As a concrete example, consider the classic motor stimuli functional activation problem: finger tapping. When you tap your thumb against your forefingers, it is well known that a very small part of the motor cortex is activated. In a recent experiment (fig. 10) we investigated whether the full hemodynamic responses associated with finger tapping could be measured non-invasively *in vivo*, through the skull. To this end, we built a small diffuse optical probe pad with multiple source-detector separations ($\sim 2.5\,\mathrm{cm}$), and with the ability to carry out both DOS and DCS measurements concurrently. We placed the probe on the heads of multiple subjects, sometimes with finger tapping on and sometimes with finger tapping off, and sometimes over the activated region of the motor cortex and sometimes a centimeter away from this activation region.

Our observations are summarized concisely in fig. 10. With the probe in the "wrong place", activation was not observed. On the other hand, with the probe placed directly over the motor activation site, we observed large perturbations in the concentrations of oxy-, deoxy-hemoglobin, and in blood flow. Averaging over a small subject population permits comparison with other techniques, and calculation of oxygen metabolism from the all-optical probe! A most exciting aspect of this work is the quantification potential

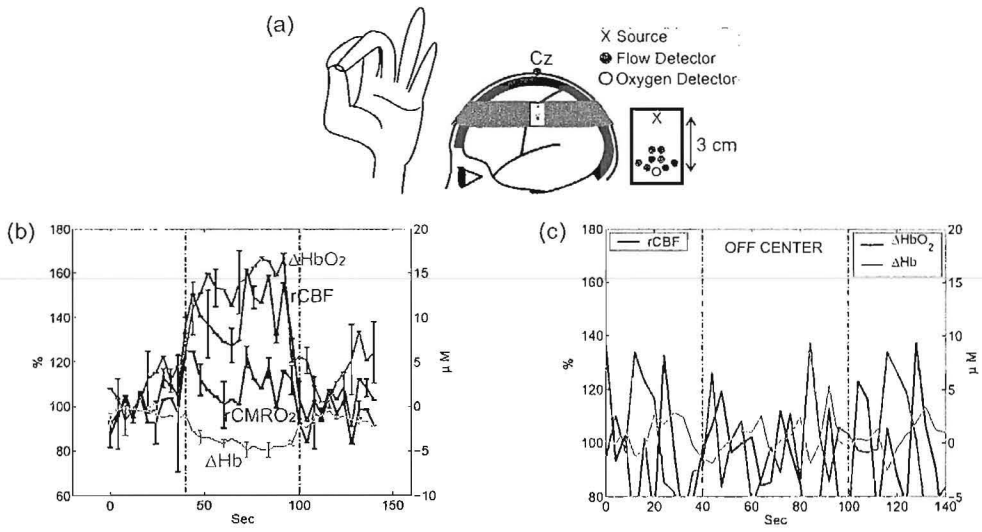

Fig. 10. – (a) Schematic diagram showing the experimental setup. Hemodynamic responses are measured by diffuse optical methods as a function of time. In (b) and (c) data between dashed lines mark activation period. (b) Data with probe located over the somatomotor cortex, and (c) 1 cm off-center from the activation spot (color online) [32].

of diffuse optics. Indeed, many researchers are exploring all sorts of functional activation paradigms with diffuse optics at the present time [43,48-52].

In considering clinical applications for brain, it is important to first reflect upon the sorts of things that doctors measure at the present time, as well as upon the kinds of physiological information that doctors need/want to know. Most of the current clinical methods focus on metabolism-related problems and issues such as oxygen delivery, pressure differences in the brain due to, for example, swelling, and flow autoregulation. In fact, many treatment strategies for brain-injured patients basically aim to increase blood flow to the injured parts of brain. For example, the normal brain has a broad range of cerebral perfusion pressure conditions for which the brain autoregulatory apparatus adjusts to keep oxygen delivery optimized. However, if a patient falls out of this normal range due to stroke or head injury, then the vasculature does not respond as well, and the patient might need drugs or other manipulations to ameliorate problems. The situation is exacerbated because the current diagnostic tools available to clinicians tend to be very invasive (*e.g.*, intracranial pressure and oxygen monitors, etc.) and/or very slow, cumbersome and costly (*e.g.*, MRI, Xe-CT, etc.). Thus a golden opportunity for diffuse optics is evident: continuous cerebral blood flow and oxygenation monitoring.

A recent study, that illustrates the potential of diffuse optics for monitoring flow treatment, was carried out in a critically ill population of ischemic stroke patients [37]. The idea of these experiments (fig. 11) was to longitudinally monitor cerebral hemodynamics at the bedside induced by changes in head-of-bed positioning. Our hypothesis

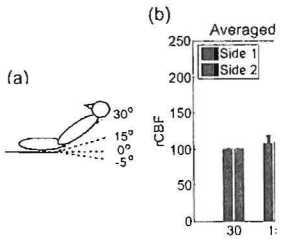

Fig. 11. – (a) Schematic
changes in each hemisphe
in diseased population sh
25% of the population pr
degrees (color online) [37

was that in response to
to larger changes in cer
to the "healthy", contr
were obtained from pat
65 years). The probes w
flow and the hemoglobi
positions of 30, 15, 0, –
clear differentiation wa
icant over the whole pc
observed that cerebral
small at this HOB ang
injury patients and wa
a parameter that is nc
example illustrates tha
of critically ill patients,
optimize patient care b

The last clinical exa
and monitoring based
optics is a relative newc
in this important field.
high and intermediate
certain classes of call-b
that the diffuse optics
higher-fidelity images
application niches.

Here again, rather t
opt to show some illustr
soft compression device
surements in transmiss

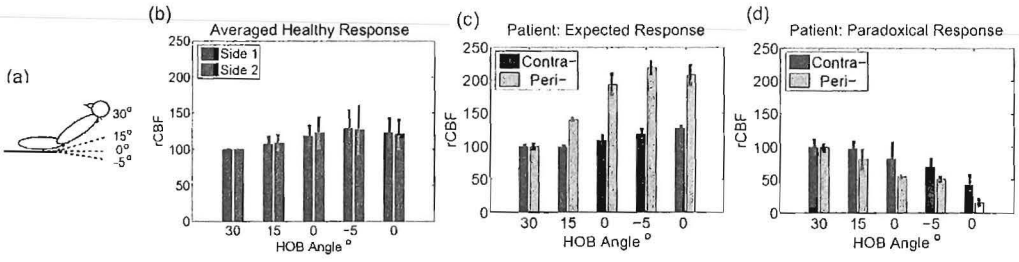

Fig. 11. – (a) Schematic representation of the head-of-bed (HOB) manipulation. (b) CBF changes in each hemisphere after each HOB manipulation in a healthy population. CBF changes in diseased population showed (c) impaired autoregulation in the injured hemisphere, but about 25% of the population presented a paradoxical response (d), where CBF was decreased at -5 degrees (color online) [37].

was that in response to this challenge, the impaired cerebral autoregulation would lead to larger changes in cerebral hemodynamics in the infarcted hemisphere by comparison to the "healthy", contralateral hemisphere. To this end, diffuse optical measurements were obtained from patients with acute hemispheric ischemic stroke ($n = 17$, mean age 65 years). The probes were placed on the forehead near the frontal poles. Cerebral blood flow and the hemoglobin concentrations were measured at different head-of-bed (HOB) positions of 30, 15, 0, -5 and 0 degrees, and normalized to their values at 30 degrees. A clear differentiation was observed between two hemispheres that was statistically significant over the whole population. Interestingly, in roughly one-fourth of the patients we observed that cerebral blood flow was not maximized at -5 degrees; rather it was very small at this HOB angle. This paradoxical response was observed in traumatic brain injury patients and was likely a result of a substantial increase in intracranial pressure, a parameter that is not routinely monitored in ischemic stroke patients. This simple example illustrates that diffuse optical instrumentation can be deployed at the bed-side of critically ill patients, and that the methodology may be promising for use as a tool to optimize patient care based on real-time cerebral hemodynamic measurements.

The last clinical example we will discuss concerns breast cancer detection, diagnosis and monitoring based (primarily) on diffuse optical tomography. Even though diffuse optics is a relative newcomer to the breast imaging field, the methodology could find uses in this important field. Potential niches for diffuse optics include detection/screening in high and intermediate risk populations, diagnosis between malignant and benign among certain classes of call-back patients, and therapy monitoring. Collectively, our view is that the diffuse optics field is just now at the point where we are starting to obtain higher-fidelity images of breast cancer, and we are beginning to confirm and identify application niches.

Here again, rather than provide a comprehensive review of the breast-DOT field, we opt to show some illustrative results from our lab [33,53-55]. We have built a parallel-plate soft compression device shown schematically in fig. 12. The instrument carries out measurements in transmission and remission at six optical wavelengths, and it is capable of

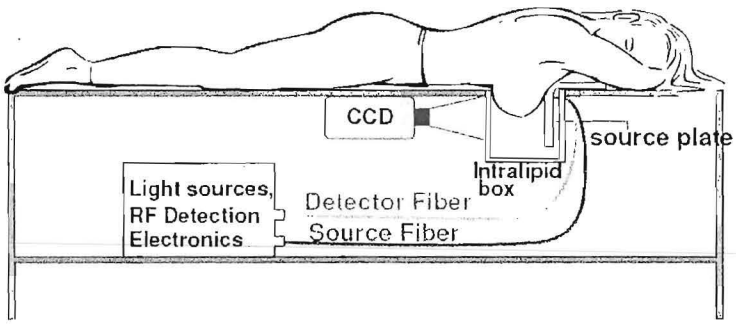

Fig. 12. – Schematic representation of the parallel-plate diffuse optical tomography instrument.

both continuous-wave and frequency-modulated measurements. Approximately 10^5–10^6 measurements are effectively performed in $\sim$ 10 minutes. These measurements are then used as input to the inverse problem, and a three-dimensional (3D) tomogram of breast tissue physiological properties is thereby obtained [56, 57].

A sample image, showing a slice out of the full 3D reconstruction, is given in fig. 13; in this case an invasive ductal carcinoma is found. Notice that the tumor shows up in some physiological variables (*e.g.* THC), but not in all (*e.g.* S_tO_2). Furthermore, optical indices based on multiple physiological/optical properties can be constructed to improve tumor-to-normal contrast. Images such as these are based on endogenous tissue contrast, which is typically relatively small (1.3× to 1.5×). Exogenous contrast agents, such as Indocyanine Green (ICG), offer the potential for improved contrast. Figure 14 shows recent images based on exogenous contrast via fluorescence-DOT and standard-DOT endogenous contrast of the same tumor; notice that the ICG contrast is substantial and is therefore likely to stimulate development of better molecular markers for tumors in the future.

Particularly in breast cancer, we expect that innovations in instrumentation and reconstruction algorithms will continue to be developed and combined to improve image fidelity and resolution. In addition, more *in vivo* breast cancer data will provide critical insight and guidance for directed algorithm/instrumentation development. In searching for enhanced differentiation between tumor and normal tissues, groups across the community are employing broader wavelength ranges to explore water, lipid and collagen concentrations, bound water fraction, and refractive index [58-60], and they are even exploring blood flow and metabolic contrast in breast cancer [33, 61]. Multi-modal imaging and monitoring approaches can potentially overcome structural resolution limitations of DOT, using the spatial information provided by other imaging modalities to constrain the DOT inverse problem. These multi-modal approaches provide extra physiological information. DOT measurements have been made with concurrent MRI [62, 63], 3D X-ray mammography [64], and ultrasound [65]. Furthermore, advances in diffuse optical tomography of breast are critical for exploitation of the advances of molecular imaging [66], an emerging field of medicine with promise of new-generation optical-contrast agents.

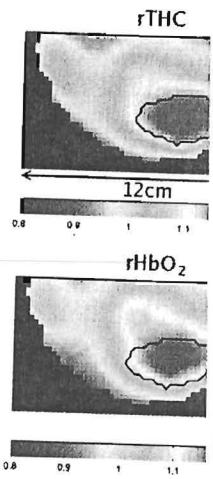

Fig. 13. – Caudal-cra
a tumoral region, wit

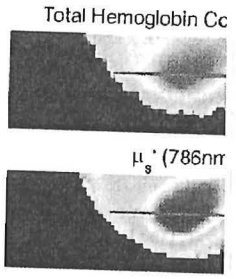

Fig. 14. – Optical ima
constrast. Notice the
rameters (see [53] for

8. – Concluding re

It should be evide
In this informal revie
left a substantial an
diffuse optics diagnos
therapy monitoring
studies of osteoarthri
inspired the reader to

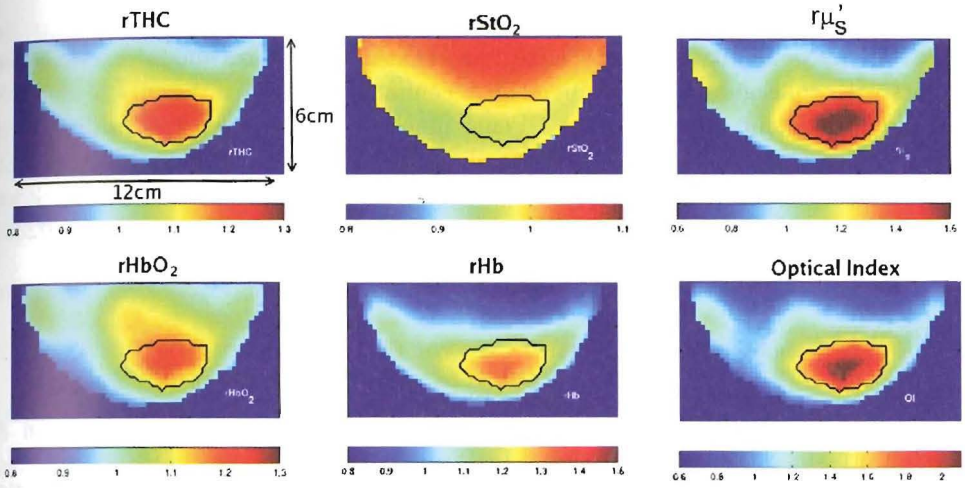

Fig. 13. – Caudal-cranial view of diffuse optical images in a field of view (black arrows) covering a tumoral region, with different parameters used as contrast [55].

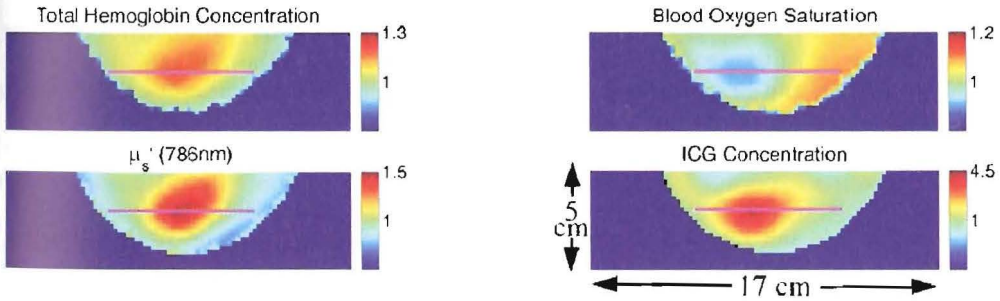

Fig. 14. – Optical images from a breast with a tumoral region, using different parameters as constrast. Notice the high contrast provided by ICG, compared to the others endogenous parameters (see [53] for more details).

8. – Concluding remarks

It should be evident that the dream of using optics for *in vivo* biopsy is being realized. In this informal review we have described these developments broadly, but we have also left a substantial amount of important research out of our discussion. For example, diffuse optics diagnostics have found uses in the study of muscle disease [36], in cancer therapy monitoring of human subjects [55] and pre-clinical animal models [67, 68], in studies of osteoarthritis [69] and skin disease [70]. We hope that our discourse will have inspired the reader to explore the field further and perhaps even to join in the fun!

* * *

The authors would like to acknowledge many fruitful discussions and interactions over the years with colleagues from the biomedical community at the University of Pennsylvania and throughout the world. At UPenn, much of this research was facilitated by sustained collaborations with B. CHANCE, J. GREENBERG, J. DETRE, M. SCHNALL, J. CULVER, G. YU, D. BOAS, T. DURDURAN, R. CHOE, and T. BUSCH. This work was supported by the National Institutes of Health through NS-060653, HL-57835, RR-02305, NS-45839, and CA-126187.

REFERENCES

[1] YODH A. and CHANCE B., *Phys. Today*, **48** (1995) 34.
[2] HIELSCHER A. H., BLUESTONE A. Y., ABDOULAEV G. S., KLOSE A. D., LASKER J., STEWART M., NETZ U. and BEUTHAN J., *Disease Markers*, **18** (2002) 313.
[3] YODH A. G. and BOAS D. A., *Functional Imaging with Diffusing Light*, in *Biomedical Photonics*, edited by VO-DINH T. (CRC Press, Boca Raton) 2003, pp. 21/1-45.
[4] OBRIG H. and VILLRINGER A., *J. Cereb. Blood Flow Metab.*, **23** (2003) 1.
[5] GIBSON A. and DEHGHANI H., *Philos. Trans R. Soc. A*, **367** (2009) 3055.
[6] WANG L. V. and WU H., *Diffuse Optical Tomography*, in *Biomedical Optics: principles and imaging* (John Wiley & Sons, New Jersey) 2007, pp. 249-282.
[7] VAN DE HULST H. C., *Light Scattering by Small Particles* (Dover, Mineola) 1981.
[8] CLARK N. A., LUNACEK J. H. and BENEDEK G. B., *Am. J. Phys.*, **38** (1970) 575.
[9] BERNE B. J. and PECORA R., *Dynamic Light Scattering with Applications to Chemistry, Biology, and Physics* (Krieger, Malabar) 1990.
[10] CHU B., *Laser Light Scattering: Basic Principles and Practice* (Academic, New York) 1991.
[11] ARRIDGE S. R. and SCHOTLAND J. C., *Inverse Problems*, **25** (2009) 123010.
[12] CASE K. M. and ZWEIFEL P. F., *Linear Transport Theory* (Addison-Wesley, Reading) 1967.
[13] ISHIMARU A., *Wave Propagation and Scattering in Random Media* (Academic Press, San Diego) 1978.
[14] O'LEARY M. A., BOAS D. A., CHANCE B. and YODH A. G., *Phys. Rev. Lett.*, **69** (1992) 2658.
[15] BOAS D. A., O'LEARY M. A., CHANCE B. and YODH A. G., *Phys. Rev. E*, **47** (1993) R2999.
[16] DANEN R. M., WANG Y., LI X. D., THAYER W. S. and YODH A. G., *Photochem. Photobiol.*, **67** (1998) 33.
[17] ARRIDGE S. R., *Inverse Problems*, **15** (1999) R41.
[18] BOAS D. A., BROOKS D. H., MILLER E. L., DIMARZIO C. A., KILMER R. J. and ZHANG Q., *IEEE Sign. Proc. Mag.*, November (2001) 57.
[19] GIBSON A. P., HEBDEN J. C. and ARRIDGE S. R., *Phys. Med. Biol.*, **50** (2005) R1.
[20] KAK A. C. and SLANEY M., *Principles of Computerized Tomographic Imaging* (IEEE Press, New York) 1988.
[21] GOLUB G. and KAHAN W., *J. SIAM Numer. Anal.*, **2** (1965) 205.
[22] ACKERSON B. J., DOUGHERTY R. L., REGUIGUI N. M. and NOBBMAN U., *J. Termophys. Heat Trans.*, **6** (1992) 577.
[23] DOUGHERTY R. L., ACKERSON B. J., REGUIGUI N. M., DORRI-NOWKOORANI F. and NOBBMAN U., *J. Quantum Spectrosc. Radiat. Transfer*, **52** (1994) 713.

[24] BOAS D. A., C
[25] BOAS D. A. an
[26] MARET G. and
[27] STEPHEN M. J.,
[28] PINE D. J., WE
(1988) 1134.
[29] BOAS D. A.,
Turbid Media:
Pennsylvania) 19
[30] CHEUNG C., CU
Med. Biol., **46** (
[31] CULVER J. P., I
A. G., *J. Cereb.*
[32] DURDURAN T.,
ZHOU C. and YO
[33] DURDURAN T., (
A. G., *Opt. Lett.*
[34] YU G., DURDUR
C. M., GLATSTE
[35] SUNAR U., QUO
KILGER A., LUST
Opt., **11** (2006) (
[36] YU G., FLOYD T
Opt. Express, **17**
[37] DURDURAN T.,
B. L., PUTT M
DETRE J. A., *O*
[38] BUCKLEY E. M.,
SCHULTZ S., SEI
YODH A. G., *O*
[39] SHERWOOD L.,
Belmont) 2006.
[40] WIDMAIER E. P
Body Function (
[41] WANG H. W., P
and BUSCH T. M
[42] DURDURAN T., *I*
Optical Methods
[43] LI J., DIETSCHE
B. and GISLER
[44] SICARD K. M. a
[45] JONES M., BERV
(2005) 609.
[46] HUPPERT T. J.,
BOAS D. A., *J.*
[47] KIM M. N., DUI
ZHOU C., YU (
GREENBERG J.
Neurocrit. Care,
[48] VILLRINGER A.

[24] BOAS D. A., CAMPBELL L. E. and YODH A. G., *Phys. Rev. Lett.*, **75** (1995) 1855.
[25] BOAS D. A. and YODH A. G., *J. Opt. Soc. Am. A*, **14** (1997) 192.
[26] MARET G. and WOLF P. E., *Z. Phys. B*, **65** (1987) 409.
[27] STEPHEN M. J., *Phys. Rev. B*, **37** (1988) 1.
[28] PINE D. J., WEITZ D. A., CHAIKIN P. M. and HERBOLZHEIMER E., *Phys. Rev. Lett.*, **60** (1988) 1134.
[29] BOAS D. A., *Diffuse Photon Probes of Structural and Dynamical Properties of Turbid Media: Theory and Biomedical Applications* (Ph.D. dissertation, University of Pennsylvania) 1996.
[30] CHEUNG C., CULVER J. P., TAKAHASHI K., GREENBERG J. H. and YODH A. G., *Phys. Med. Biol.*, **46** (2001) 2053.
[31] CULVER J. P., DURDURAN T., FURUYA D., CHEUNG C., GREENBERG J. H. and YODH A. G., *J. Cereb. Blood Flow Metab.*, **23** (2003) 911.
[32] DURDURAN T., YU G., BURNETT M. G., DETRE J. A., GREENBERG J. H., WANG J., ZHOU C. and YODH A. G., *Opt. Lett.*, **29** (2004) 1766.
[33] DURDURAN T., CHOE R., YU G., ZHOU C., TCHOU J. C., CZERNIECKI B. J. and YODH A. G., *Opt. Lett.*, **30** (2005) 2915.
[34] YU G., DURDURAN T., ZHOU C., WANG H. W., PUTT M. E., SAUNDERS M., SEGHAL C. M., GLATSTEIN E., YODH A. G. and BUSCH T. M., *Clin. Cancer Res.*, **11** (2005) 3543.
[35] SUNAR U., QUON H., DURDURAN T., ZHANG J., DU J., ZHOU C., YU G., CHOE R., KILGER A., LUSTIG R., LOEVNER L., NIOKA S., CHANCE B. and YODH A. G., *J. Biomed. Opt.*, **11** (2006) 064021.
[36] YU G., FLOYD T., DURDURAN T., ZHOU C., WANG J. J., DETRE J. A. and YODH A. G., *Opt. Express*, **17** (2007) 1064.
[37] DURDURAN T., ZHOU C., EDLOW B. L., YU G., CHOE R., KIM M. N., CUCCHIARA B. L., PUTT M. E., SHAH Q., KASNER S. E., GREENBERG J. H., YODH A. G. and DETRE J. A., *Opt. Express*, **17** (2009) 3884.
[38] BUCKLEY E. M., COOK N. M., DURDURAN T., KIM M. N., ZHOU C., CHOE R., YU G., SCHULTZ S., SEHGAL C. M., LICHT D. J., ARGER P. H., PUTT M. E., HURT H. H. and YODH A. G., *Opt. Express*, **17** (2009) 12571.
[39] SHERWOOD L., *Fundamentals of Physiology: A Human Perspective* (Thomson Brooks, Belmont) 2006.
[40] WIDMAIER E. P., RAFF H. and STRANG K. T., *Human Physiology: The Mechanisms of Body Function* (McGraw-Hill, Los Angeles) 2007.
[41] WANG H. W., PUTT M. E., EMANUELE M. J., SHIN D. B., GLATSTEIN E., YODH A. G. and BUSCH T. M., *Cancer Res.*, **64** (2004) 7553.
[42] DURDURAN T., *Non-Invasive Measurements of Tissue Hemodynamics with Hybrid Diffuse Optical Methods* (Ph.D. dissertation, University of Pennsylvania) 2004.
[43] LI J., DIETSCHE G., IFTIME D., SKIPETROV S. E., MARET G., ELBERT T., ROCKSTROH B. and GISLER T., *J. Biomed. Opt.*, **10** (2005) 044002.
[44] SICARD K. M. and DUONG T. Q., *Neuroimage*, **25** (2005) 850.
[45] JONES M., BERWICK J., HEWSON-STOATE N., GIAS C. and MAYHEW J., *Neuroimage*, **27** (2005) 609.
[46] HUPPERT T. J., JONES P. B., DEVOR A., DUNN A. K., TENG I. C., DALE A. M. and BOAS D. A., *J. Biomed. Opt.*, **14** (2009) 044038.
[47] KIM M. N., DURDURAN T., FRANGOS S., EDLOW B. L., BUCKLEY E. M., MOSS H. E., ZHOU C., YU G., CHOE R., MALONEY-WILENSKY E., WOLF R. L., GRADY M. S., GREENBERG J. H., LEVINE J. M., YODH A. G., DETRE J. A. and KOFKE W. A., *Neurocrit. Care*, **12** (2010) 173.
[48] VILLRINGER A. and CHANCE B., *Trends Neurosc.*, **20** (1997) 435.

[49] FRANCESCHINI M. A., THAKER S., THEMELIS G., KRISHNAMOORTHY K. K., BORTFELD H., DIAMOND S. G., BOAS D. A., ARVIN K. and GRANT P. E., *Pediatr. Res.*, **61** (2007) 546.
[50] ZEFF B. W., WHITE B. R., DEHGHANI H., SCHLAGGAR B. L. and CULVER J. P., *Proc. Natl. Acad. Sci. U.S.A.*, **104** (2007) 12169.
[51] JAILLON F., LI J., DIETSCHE G., ELBERT T. and GISLER T., *Opt. Express*, **15** (2007) 6643.
[52] BECERRA L., HARRIS W., JOSEPH D., HUPPERT T., BOAS D. A. and BORSOOK D., *Neuroimage*, **41** (2008) 252.
[53] CORLU A., CHOE R., DURDURAN T., ROSEN M. A., SCHWEIGER M., ARRIDGE S. R. and YODH A. G., *Opt. Express*, **15** (2007) 6696.
[54] KONECKY S. D., CHOE R., CORLU A., LEE K., WIENER R., SRINIVAS S. M., SAFFER J. R., FREIFELDER R., KARP J. S., HAJJIOUI N., AZAR F. and YODH A. G., *Med. Phys.*, **35** (2008) 446.
[55] CHOE R., KONECKY S. D., CORLU A., LEE K., DURDURAN T., BUSCH D. R., PATHAK S., CZERNIECKI B. J., TCHOU J., FRAKER D. L., DEMICHELE A., CHANCE B., ARRIDGE S. R., SCHWEIGER M., CULVER J. P., SCHNALL M. D., PUTT M. E., ROSEN M. A. and YODH A. G., *J. Biomed. Opt.*, **14** (2009) 024020.
[56] ARRIDGE S. R. and SCHWEIGER M., *Appl. Opt.*, **34** (1995) 8026.
[57] ARRIDGE S. R. and SCHWEIGER M., *Opt. Express*, **2** (1998) 213.
[58] SRINIVASAN S., POGUE B. W., BROOKSBY B., JIANG S., DEHGHANI H., KOGEL C., WELLS W. A., POPLACK S. P. and PAULSEN K. D., *Technol. Cancer Res. Treat.*, **4** (2005) 513.
[59] CERUSSI A., SHAH N., HSIANG D., DURKIN A., BUTLER J. and TROMBERG B. J., *J. Biomed. Opt.*, **11** (2006) 044005.
[60] SRINIVASAN S., POGUE B. W., CARPENTER C., JIANG S., WELLS W. A., POPLACK S. P., KAUFMAN P. A. and PAULSEN K. D., *Antioxidants Redox Signaling*, **9** (2007) 1143.
[61] ZHOU C., CHOE R., SHAH N., DURDURAN T., YU G., DURKIN A., HSIANG D., MEHTA R., BUTLER J., CERUSSI A., TROMBERG B. J. and YODH A. G., *J. Biomed. Opt.*, **12** (2007) 051903.
[62] NTZIACHRISTOS V., YODH A. G., SCHNALL M. D. and CHANCE B., *Neoplasia*, **4** (2002) 347.
[63] CARPENTER C. M., SRINIVASAN S., POGUE B. W. and PAULSEN K. D., *Opt. Express*, **16** (2008) 17903.
[64] FANG Q., CARP S. A., SELB J., BOVERMAN G., ZHANG Q., KOPANS D. B., MOORE R. H., MILLER E. L., BROOKS D. H. and BOAS D. A., *IEEE Trans. Med. Imaging*, **28** (2009) 30.
[65] ZHU Q., TANNENBAUM S., HEGDE P., KANE M., XU C. and KURTZMAN S. H., *Neoplasia*, **10** (2008) 1028.
[66] WEISSLEDER R. and NTZIACHRISTOS V., *Nature Med.*, **9** (2003) 123.
[67] LUCKL J., ZHOU C., DURDURAN T., YODH A. G. and GREENBERG J. H., *J. Neurosci. Res.*, **87** (2009) 1219.
[68] ZHOU C., EUCKER S. A., DURDURAN T., YU G., RALSTON J., FRIESS S. H., ICHORD R. N., MARGULIES S. S. and YODH A. G., *J. Biomed. Opt.*, **14** (2009) 034015.
[69] HOFMANN G. O., MARTICK J., GROSSTUCK R., HOFFMANN M., LANGE M., PLETTENBERG H. K. W., BRAUNSHWEIG R., SCHILLING O., KADEN I. and SPAHN G., *Pathophysiol.*, **17** (2010) 1.
[70] BEDNOV A., ULYANOV S., CHEUNG C. and YODH A. G., *J. Biomed. Opt.*, **9** (2004) 347.